MAP PROJECTIONS BETWEEN ARBITRARY EUCLIDEAN AND SPHERICAL POLYGONS

B R S RECHT

Contents

1. Introduction

A small but persistent trend in creating world maps has been to map onto a polyhedron, and then unfold the polyhedron into a flat polyhedral net. Most maps in this category use regular polyhedra, often the cube or the icosahedron (in Fuller's second Dymaxion map).[9] Other polyhedra include the other regular solids and some Archimedean solids; Fuller used the cuboctahedron for his first Dymaxion map,[10] and the truncated icosahedron was used by Snyder.[22] Maps between a polygon and a hemisphere can be considered as polyhedral maps if the dihedron is allowed.[23][12] The inverse mapping can be used to inscribe a grid on a sphere, as in the quadrilateralized spherical cube[1][16] or discrete global grids.[20]

Discussion of these maps often neglects the projection used to project onto the polyhedron. For this paper, we'll limit ourselves to projections that map a certain spherical polygon to a Euclidean polygon. (Some projections, like HEALPix, have some edges that correspond to small circles on the sphere: we leave those out). In the literature, there are four such map projections (or families thereof) that are often used:

- Gnomonic - Known in antiquity, this map projection preserves geodesics: great circle arcs on the sphere are mapped to lines on the plane.
- Conformal - These map projections preserve the shape of features.

Date: July 2019.

Name	Polygons	To plane	To sphere	Notes
Gnomonic	All contained within a hemisphere			Preserves geodesics
Conformal	Triangles less than or equal to hemisphere	Eq. 27	Eq. 27	In theory higher polygons, but no general formula
Equal-area	Any regular polygon less than or equal to hemisphere (maybe more)?	Ref. [22] page 13	Ref. [22] pages 13–14	Not differentiable along lines from vertices to center
Areal	Triangles less than hemisphere			Unusual result on full hemisphere
Fuller	Triangles less than hemisphere? Quadrilaterals less than hemisphere?			[11][9][10]
Naive slerp	Triangles less than or equal to hemisphere	NI	Eq. 40	Parameterized
	Quadrilaterals less than or equal to hemisphere	NI	Eq. 42, Eq. 44	Parameterized
Elliptical	Quadrilaterals with equal angles less than or equal to hemisphere	NI	Eq. 52	Parameterized

Table 1. Map projections in this text. Ω is the area of the spherical polygon. NI = numerical inversion.

- Equal-Area - These map projections preserve the relative area of features.[22]
- Fuller - The map projections derived by Buckminster Fuller for his Dymaxion maps.[9][10][2]

These will be discussed in more detail later on. There are also map projections in the literature for particular polygons, e.g. the faces of a particular regular polyhedron like a cube or icosahedron. These won't be mentioned except when they fall into one of the families above.

There are two sources outside of the study of geography that will be drawn on in this text. One is Buckminster Fuller's construction of geodesic domes, where a method analogous to the Fuller projection appears.[11] Another is the field of computer graphics, where there is some interest in functions between the square to the disk.[4][7] These functions can be composed with an appropriate map projection from the disk to the hemisphere to create a map projection between the square and the sphere.[12]

Nearly all of the literature on map projections between Euclidean and spherical polygons, either in general or particular, only deals with regular polygons. However, geographical features do not follow any regular geometric rules. Regular polygons are mathematically easier to study, but irregular polygons are also tractable. In this text, map projections between general Euclidean and spherical polygons will be described. Some of these are extensions of existing map projections, while some are new compromise map projections.

2. Preliminaries

Let (u, v) be a vector in $\mathbb{R}^2$, and $\zeta = u + iv$ be the corresponding complex number in $\mathbb{C}$ or the Riemann sphere $\mathbb{C} \cup \{\infty\}$. Which notation is used will depend on the mapping: conformal maps are best expressed in terms of complex variables.

2.1. **Spherical geometry with 3-vectors.**

Some of the map projections to be discussed are better expressed in terms of a vector rather than latitude and longitude. This text will only cover pertinent details: a fuller description can be found in e.g. [8].

Let $\phi \in [-\frac{\pi}{2}, \frac{\pi}{2}]$ be latitude, and $\lambda \in (-\pi, \pi]$ be longitude. Let $\mathbf{v} = (x, y, z)$ be a vector in $\mathbb{R}^3$ and $\hat{\mathbf{v}} = (x, y, z)$ be a unit vector on the sphere S^2 such that $\|\hat{\mathbf{v}}\| = \sqrt{x^2 + y^2 + z^2} = 1$. To convert from latitude and longitude to a unit vector:

$$\hat{\mathbf{v}} = (\sin(\phi), \sin(\lambda)\cos(\phi), -\cos(\lambda)\cos(\phi)) \tag{1}$$

To convert from the unit vector $\hat{\mathbf{v}}$ to latitude and longitude:

$$\begin{aligned} \phi &= \arcsin(x) = \arctan(x, \sqrt{y^2+z^2}) \\ \lambda &= \arctan(y, -z) \end{aligned} \tag{2}$$

Often in this text we'll normalize a vector to make it a unit vector. For brevity, we'll notate this pre-normalized vector as $\widetilde{\mathbf{v}}$, such that

$$\hat{\mathbf{v}} = \frac{\widetilde{\mathbf{v}}}{\|\widetilde{\mathbf{v}}\|} \tag{3}$$

2.1.1. *Great circles.* The shortest distance (geodesic) between two points in Euclidean space is a straight line. On the sphere, the shortest distance is an arc of the great circle between those points. That distance is the central angle θ between the two points. There are a few vector forms for it, the most numerically stable one being the one using arctan.

$$\begin{aligned} \theta &= \arccos\left(\hat{\mathbf{v}}_1 \cdot \hat{\mathbf{v}}_2\right) \\ &= \arcsin\left(\|\hat{\mathbf{v}}_1 \times \hat{\mathbf{v}}_2\|\right) \\ &= \arctan\left(\frac{\|\hat{\mathbf{v}}_1 \times \hat{\mathbf{v}}_2\|}{\hat{\mathbf{v}}_1 \cdot \hat{\mathbf{v}}_2}\right) \end{aligned} \tag{4}$$

The great circle is the intersection of the sphere and a plane passing through the origin. A plane through the origin can be specified as $\hat{\mathbf{n}} \cdot \mathbf{v} = 0$, where $\hat{\mathbf{n}}$ is a unit vector normal to the plane; this vector $\hat{\mathbf{n}}$ can be used to specify a great circle. Given two points $\hat{\mathbf{v}}_\mathbf{1}, \hat{\mathbf{v}}_\mathbf{2}$ on the sphere, the $\hat{\mathbf{n}}$ of the great circle between those two points is (up to normalization) their cross product:

$$\widetilde{\mathbf{n}} = \hat{\mathbf{v}}_1 \times \hat{\mathbf{v}}_2 \tag{5}$$

Two great circles intersect at two antipodal points on the sphere. The points of intersection can be found as the cross product of the great circle normals:

$$\widetilde{\mathbf{v}} = \pm\hat{\mathbf{n}}_\mathbf{1} \times \hat{\mathbf{n}}_2 \tag{6}$$

2.1.2. *Interpolation.* Interpolation in Euclidean space is standard linear interpolation. On the sphere, interpolation is given by spherical linear interpolation, or slerp.

$$\operatorname{Lerp}(\mathbf{v_1}, \mathbf{v_2}; t) = (1-t)\mathbf{v_1} + t\mathbf{v_2} \tag{7}$$

$$\operatorname{Slerp}(\hat{\mathbf{v}}_\mathbf{1}, \hat{\mathbf{v}}_\mathbf{2}; t) = \frac{\sin((1-t)w)}{\sin(w)}\hat{\mathbf{v}}_\mathbf{1} + \frac{\sin(tw)}{\sin(w)}\hat{\mathbf{v}}_\mathbf{2} \tag{8}$$

where $w = \arccos \hat{\mathbf{v}}_\mathbf{1} \cdot \hat{\mathbf{v}}_\mathbf{2}$. If $\hat{\mathbf{v}}_\mathbf{1} = \hat{\mathbf{v}}_\mathbf{2}$, then define $\operatorname{Slerp}(\hat{\mathbf{v}}_\mathbf{1}, \hat{\mathbf{v}}_\mathbf{2}; t) = \hat{\mathbf{v}}_\mathbf{1} = \hat{\mathbf{v}}_\mathbf{2}$ for all t.

2.1.3. *Face normal.* For the purposes of this text, we define the normal to a (Euclidean) polygon as so, where n is the number of vertices in the polygon and $i = 0 \ldots n-1$ is an index for each vertex:

$$\widetilde{\mathbf{n}} = \sum_{i}^{n-1} \mathbf{v}_i \times \mathbf{v}_{i+1} \tag{9}$$

i should be treated as if it's mod n, so that it loops around. This definition allows for a somewhat sensible extension to skew polygons: the normal points in a generally reasonable direction when applied to a skew polygon. The normal will be outward-facing if the points are ordered counterclockwise, and inward-facing if the points are ordered clockwise.

2.2. **Euclidean spaces and transformations, including barycentric and uv coordinates.** This text uses barycentric coordinates on Euclidean triangles. Quadrilaterals are instead specified by *uv coordinates* where u and v are $\in [-1, 1]$. The subset of the plane $[-1, 1]^2$ is termed the standard square. Here we discuss transformations of those

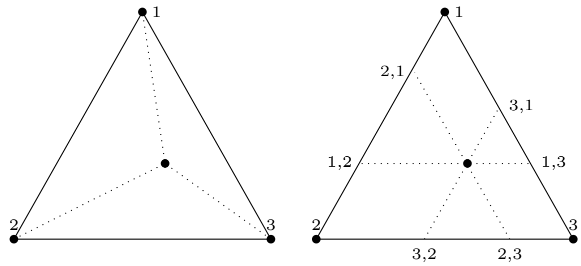

FIGURE 1. Barycentric coordinates. Left: Area opposite of each vertex. Right: Intersection of lines parallel with triangle edges.

2.2.1. *Affine transformation.* Affine transformations are combinations of reflection, scaling, rotation, shearing, and translation. This can be expressed as $\mathbf{v} = \mathbf{A}[u, v]^T + v_0$, where $\mathbf{A}$ is a matrix. However, it is often more convenient to express affine transformations using an augmented matrix like so:

$$\begin{bmatrix} x \\ y \\ 1 \end{bmatrix} = \mathbf{M} \begin{bmatrix} u \\ v \\ 1 \end{bmatrix}, \mathbf{M} = \begin{bmatrix} A_{11} & A_{12} & v_{0x} \\ A_{21} & A_{22} & v_{0y} \\ 0 & 0 & 1 \end{bmatrix} \tag{10}$$

The transformation is invertible if $\mathbf{M}$ (or $\mathbf{A}$) is invertible. This transformation can also transform between spaces of different dimension, although then $\mathbf{M}$ is not a square matrix.

Affine transformations are equal-area in the sense defined earlier if $|\mathbf{M}| \neq 0$, so if using an equal-area projection it may be desirable to limit oneself to affine transformations. If $|\mathbf{M}| = 1$, then it defines a conformal affine transformation, effectively a combination of translation and rotation.

2.2.2. *Barycentric coordinates.* Barycentric coordinates are in fact a special kind of affine coordinates. Barycentric coordinates are real numbers $\beta_1, \beta_2, \beta_3$ such that $\sum_{i=1}^3 \beta_i = 1$. Given a triangle with vertices $\mathbf{v}_1, \mathbf{v}_2, \mathbf{v}_3$, the corresponding vertex is given by $\mathbf{v} = \sum_{i=1}^3 \beta_i \mathbf{v}_i$. Given $\mathbf{v}$ and $\mathbf{v}_i$, β_i can be found by e.g. solving the linear system of $\beta_1 + \beta_2 + \beta_3 = 1$ and $\mathbf{v} = \sum_{i=1}^3 \beta_i \mathbf{v}_i$. β_i are all positive on the interior of the triangle. If a point lies on an edge opposite vertex i, then β_i is zero. (If it lies beyond the edge, then $\beta_i < 0$.)

There are two geometric interpretations of barycentric coordinates that will be useful, as depicted in Figure 1. One is that β_i is the area of the smaller triangle opposite $\mathbf{v}_i$ divided by the area of the large triangle. The other is that if a line is placed passing through $\mathbf{v}$ parallel to the edge opposite vertex i, it will be at β_i of the distance between the edge and its opposite vertex, with $\beta_i = 0$ being on the edge itself. Let $\mathbf{v}_{i,j}$ be the point where the line for i meets the line between vertices i and j: then the vertex lies $\frac{\beta_j}{1-\beta i}$ of the distance from $\mathbf{v}_{i,j}$ to $\mathbf{v}_{i,j+1}$. Symbolically, $\mathbf{v}_{i,j} = \mathrm{Lerp}(\mathbf{v}_j, \mathbf{v}_i; \beta_i)$, and $\mathbf{v} = \mathrm{Lerp}(\mathrm{Lerp}(\mathbf{v}_{i-1}, \mathbf{v}_i; \beta_i), \mathrm{Lerp}(\mathbf{v}_{i+1}, \mathbf{v}_i; \beta_i); \frac{\beta_{i-1}}{1-\beta_i})$ for all i.

Generalized barycentric coordinates are defined similarly, but the requirement that $\sum_{i=1}^3 \beta_i = 1$ is dropped. For instance, generalized barycentric coordinates β_i' on the unit sphere replace that requirement with the condition that $\| \sum_{i=1}^3 \beta_i' \mathbf{v}_i \| = 1$. $\sum_{i=1}^3 \beta_i'$ are > 1 on the interior of the triangle, $= 1$ on the edges, and < 1 on the exterior.

2.2.3. *Homography.* Homography, or projective transformation, is commonly used in computer vision and graphics to handle objects seen in perspective, and may be convenient in some software environments. A homography may be given by:

$$\begin{bmatrix} xt \\ yt \\ t \end{bmatrix} = \mathbf{M} \begin{bmatrix} u \\ v \\ 1 \end{bmatrix} \tag{11}$$

where $\mathbf{M}$ is called the matrix of the homography. The matrix is defined up to multiplication by a positive constant: $\mathbf{M}$ and $k\mathbf{M}$ where $k > 0$ define the same homography. The inverse of this transformation is also

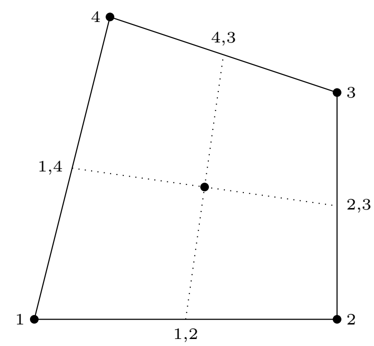

FIGURE 2. Bilinear interpolation, showing intersection of lines.

a projective transformation, with matrix of the homography $\mathbf{M}^{-1}$. Given 4 points in the uv plane and their target in the xy plane, $\mathbf{M}$ can be determined as the null-space of this system:

$$\begin{bmatrix} x_1 & x_1u_1 & x_1v_1 & -1 & -u_1 & -v_1 & 0 & 0 & 0 \\ x_2 & x_2u_2 & x_2v_2 & -1 & -u_2 & -v_2 & 0 & 0 & 0 \\ x_3 & x_3u_3 & x_3v_3 & -1 & -u_3 & -v_3 & 0 & 0 & 0 \\ x_4 & x_4u_4 & x_4v_4 & -1 & -u_4 & -v_4 & 0 & 0 & 0 \\ y_1 & y_1u_1 & y_1v_1 & 0 & 0 & 0 & -1 & -u_1 & -v_1 \\ y_2 & y_2u_2 & y_2v_2 & 0 & 0 & 0 & -1 & -u_2 & -v_2 \\ y_3 & y_3u_3 & y_3v_3 & 0 & 0 & 0 & -1 & -u_3 & -v_3 \\ y_4 & y_4u_4 & y_4v_4 & 0 & 0 & 0 & -1 & -u_4 & -v_4 \end{bmatrix} \begin{bmatrix} M_{11} \\ M_{12} \\ M_{13} \\ M_{21} \\ M_{22} \\ M_{23} \\ M_{31} \\ M_{32} \\ M_{33} \end{bmatrix} = \mathbf{0}, \tag{12}$$

where

$$\mathbf{M} = \begin{bmatrix} M_{11} & M_{12} & M_{13} \\ M_{21} & M_{22} & M_{23} \\ M_{31} & M_{32} & M_{33} \end{bmatrix}. \tag{13}$$

This transformation can also be adapted to a transform from 2-d uv space to a plane in 3-d xyz space. The target points must be coplanar, and since the matrix of the homography is now a 3 by 4 matrix, the inverse transformation is given by the pseudoinverse instead. Homographies are undefined along the line where $t = 0$, but this rarely becomes an issue in the context of this text.

2.2.4. *Bilinear Interpolation.* Another transformation is usually called 'bilinear interpolation' in image processing applications. Let $\mathbf{v}_1, \mathbf{v}_2, \mathbf{v}_3, \mathbf{v}_4$ be points in 2-d or 3-d (or higher) space. Define:

$$\begin{aligned} \mathbf{v}_{1,2} &= \mathrm{Lerp}(\mathbf{v}_1, \mathbf{v}_2; \frac{u+1}{2}), \\ \mathbf{v}_{4,3} &= \mathrm{Lerp}(\mathbf{v}_4, \mathbf{v}_3; \frac{u+1}{2}), \\ \mathbf{v}_{1,4} &= \mathrm{Lerp}(\mathbf{v}_1, \mathbf{v}_4; \frac{v+1}{2}), \\ \mathbf{v}_{2,3} &= \mathrm{Lerp}(\mathbf{v}_2, \mathbf{v}_3; \frac{v+1}{2}) \end{aligned} \tag{14}$$

Then bilinear interpolation determines the point $\mathbf{v}$ as:

$$\begin{aligned}\mathbf{v} &= \mathrm{Lerp}(\mathbf{v}_{1,2}, \mathbf{v}_{4,3}; \frac{v+1}{2}) \\ &= \mathrm{Lerp}(\mathbf{v}_{1,4}, \mathbf{v}_{2,3}; \frac{u+1}{2}) \\ &= \frac{(1-u)(1-v)}{4}\mathbf{v}_1 + \frac{(1+u)(1-v)}{4}\mathbf{v}_2 + \frac{(1+u)(1+v)}{4}\mathbf{v}_3 + \frac{(1-u)(1+v)}{4}\mathbf{v}_4 \\ &= \mathbf{a} + u\mathbf{b} + v\mathbf{c} + uv\mathbf{d}\end{aligned} \tag{15}$$

where

$$\begin{aligned}\mathbf{a} &= \frac{\mathbf{v}_1 + \mathbf{v}_2 + \mathbf{v}_3 + \mathbf{v}_4}{4}, \\ \mathbf{b} &= \frac{-\mathbf{v}_1 + \mathbf{v}_2 + \mathbf{v}_3 - \mathbf{v}_4}{4}, \\ \mathbf{c} &= \frac{-\mathbf{v}_1 - \mathbf{v}_2 + \mathbf{v}_3 + \mathbf{v}_4}{4}, \\ \mathbf{d} &= \frac{\mathbf{v}_1 - \mathbf{v}_2 + \mathbf{v}_3 - \mathbf{v}_4}{4}\end{aligned} \tag{16}$$

The uv term in the transformation illustrates the choice of name: in 3d, if the vertices v_i are not coplanar, then the transformation maps the plane to a hyperbolic paraboloid. Bilinear interpolation preserves evenly spaced points along an edge of the quadrilateral defined by v_i, and avoids the undefined space of the homography. However, the inverse function is somewhat more complicated. The inverse of bilinear interpolation, for $\mathbf{v}_i \in \mathbb{R}^2$, is given by:

$$\begin{aligned}u &= \frac{-b_u + \sqrt{b_u^2 - 4a_u c_u}}{2a_u} \\ v &= \frac{-b_v + \sqrt{b_v^2 - 4a_v c_v}}{2a_v} \\ a_u &= \mathbf{b} \times \mathbf{d}, b_u = \mathbf{a} \times \mathbf{d} + \mathbf{b} \times \mathbf{c}, c_u = \mathbf{a} \times \mathbf{c}, \\ a_v &= \mathbf{c} \times \mathbf{d}, b_v = \mathbf{a} \times \mathbf{d} - \mathbf{b} \times \mathbf{c}, c_v = \mathbf{a} \times \mathbf{b},\end{aligned} \tag{17}$$

where the 2d scalar cross product $\mathbf{a} \times \mathbf{b} = a_x b_y - b_x a_y$ is used here. In more than two dimensions, pick two coordinates and use those as x and y.

If the shape is a planar parallelogram (or a special case of a parallelogram like a rectangle), then $\mathbf{v}_1 + \mathbf{v}_3 = \mathbf{v}_2 + \mathbf{v}_4$, and $\mathbf{d} = 0$. In this case, both the homography and the hyperbolic paraboloid transformation reduce to an affine transformation. Qualitatively, homographies preserve all lines, while bilinear interpolation preserves lines of constant u or v.

Neither homographies nor bilinear interpolation are amenable to generalization in the way that barycentric coordinates are. Bilinear interpolation can be expressed like so:

$$\mathbf{v} = \sum_{i=1}^{4} \alpha_i \mathbf{v}_i, \tag{18}$$

but α_i are not necessarily unique for a given $\mathbf{v}$. Later we will see some map projections that are similar in form to bilinear interpolation.

2.3. **Dealing with the ellipsoid.** The Earth is reasonably approximated as a sphere, and better approximated as a slightly flattened oblate ellipsoid. In general this text will only deal with the spherical approximation, but here we mention two considerations arising from that approximation.

The vector form described in [8] corresponds to the geodetic latitude. The mapping between the sphere and the ellipsoid using geodetic latitude is not area-preserving, conformal, or distance-preserving, although the distortion is small on the Earth ellipsoid. If applying an area-preserving, conformal, or distance-preserving map projection, and the required precision is fine enough that the distortion is a concern, the geodetic latitude can be substituted with the authalic (equal-area), conformal, or rectifying (equal-distance along meridians)

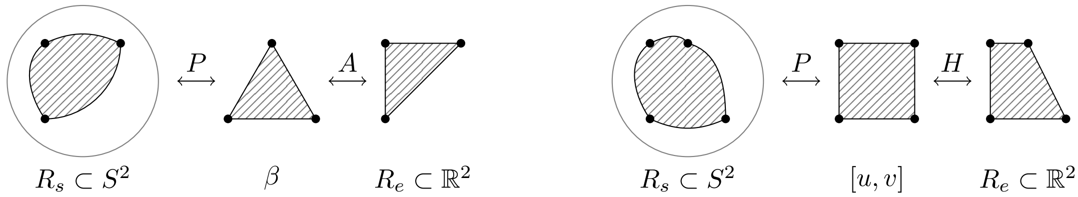

FIGURE 3. Schematic for the application of most projections listed in this text. Left: triangles, right: quadrilaterals. P indicates the projection, A is an affine transformation, and H is a homography or bilinear interpolation.

latitude as described in [21]. These can be calculated from the geodetic latitude, and the difference is well-approximated by a Fourier series.

Considering polyhedral maps, in this text we require the edges of the polyhedra to correspond to geodesics. Geodesics on a sphere are not necessarily geodesics on an ellipse: as proof, geodesics on an ellipse are not necessarily closed, while geodesics on a sphere are. (Of course, with the Earth ellipsoid, the difference between the geodesics is small.) The equator and meridians are geodesics on both surfaces, so if having exact geodesics is a concern, place your polyhedron edges along the equator or meridians.

3. Map projections

Figure 3 illustrates the general form of application of most projections in this text. (Exceptions are noted in the relevant sections.) The transformation from barycentric coordinates to the plane, or from uv coordinates to a quadrilateral, takes the same form for each projection, so in this section we can ignore that part except when there are special considerations.

The polygon on the sphere R_s and the polygon in the plane R_e can be basically anything, within the operating parameters of the projection and any special considerations that may apply. Even with respect to each other, one can be a regular polygon while the other is some irregular monster, if that is desirable. Of course, this will influence the distortion of the map projection.

The flip side of this freedom is that there is not necessarily a unique way, given R_s, to choose R_e. If one is regular, it may make sense to choose the other to also be regular. For irregular triangles, one choice may be to choose R_e such that its edges are proportial in length to those of R_s. Another may be to choose R_e to have angles proportional to those of R_s: $\alpha' = \pi\frac{\alpha}{\alpha+\beta+\gamma}$ etc. For quadrilaterals, it may be desirable to carry over some quality from R_s to R_e, but that may not uniquely define R_e: for instance, a quadrilateral is not uniquely defined (up to congruence) by its edge lengths alone, or its angles alone. In some cases, extra conditions make the choice more obvious: for example, if the spherical quadrilateral has equal sides and equal angles, it makes sense to map it to a square. If the goal is to minimize overall distortion, one may choose R_e with that in mind. In the absence of guiding conditions, aesthetics may be the best guide.

3.1. **Gnomonic.**

The gnomonic projection was known to the ancient Greeks, and is the simplest of the transformations listed here.[21] It has the property that arcs of great circles are transformed into lines on the plane and vice versa: that is, geodesics stay geodesics, and (spherical) polygons stay polygons. This projection is called Method 1 in geodesic dome terminology.[11] The main downside of the gnomonic projection is heavy distortion away from the center of the projection.

We'll describe this projection in vector form, which is a little unconvential but will allow us to compare it to other projections later. Let $\mathbf{p}$ be a point on a plane given in Hessian normal form by $\hat{\mathbf{n}} \cdot \mathbf{p} = r$. r can be any value except 0. The gnomonic projection can be described as so:

$$\widetilde{\mathbf{v}} = \mathbf{p} \tag{19}$$

$$\mathbf{p} = \frac{r}{\hat{\mathbf{n}} \cdot \hat{\mathbf{v}}}\hat{\mathbf{v}} \tag{20}$$

Projection from Euclidean space to the sphere is literally just normalizing the vector.

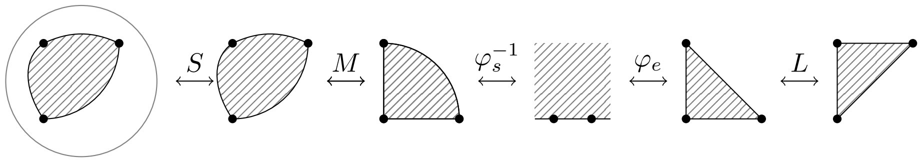

FIGURE 4. Schematic of the conformal triangular projection. S is the stereographic projection, M is a Möbius transformation, φ is the Schwarz triangle function, $\mathbb{C}^+$ is the complex upper half-plane, and L is a complex affine transformation.

For triangles, this projection can be expressed directly in terms of barycentric coordinates.

$$\widetilde{\mathbf{v}} = \beta_1 \mathbf{v}_1 + \beta_2 \mathbf{v}_2 + \beta_3 \mathbf{v}_3 \tag{21}$$

where β_i are (planar) barycentric coordinates. If the generalized coordinates are β_i', then $\beta_i' = \frac{\beta_1}{\|\beta_1 \mathbf{v}_1 + \beta_2 \mathbf{v}_2 + \beta_3 \mathbf{v}_3\|}$.

For the inverse, solve this linear system:

$$\begin{bmatrix} \mathbf{v}_1 & \mathbf{v}_2 & \mathbf{v}_3 \end{bmatrix} \beta' = \hat{\mathbf{v}} \tag{22}$$

where β' is a vector of generalized barycentric coordinates. Then obtain β as $\beta = \frac{\beta'}{\sum \beta_i'}$.

3.2. **Conformal triangular.** Here we take a turn, as this mapping is very different from the others and uses its own notation. Conformal map projections have deep connections to the theory of complex functions. Here we introduce a number of functions which will later be composed together as illustrated in Figure 4.

The stereographic projection S is the conformal map projection between the Riemann sphere $\mathbb{C} \cup \{\infty\}$ and the sphere S^2. Let $\hat{\mathbf{v}}_0$ designate the center point of the projection, to be mapped to 0 in the complex plane. Then $\zeta = S(\hat{\mathbf{v}}_0; \hat{\mathbf{v}})$. As the stereographic projection is one of the most common projections, its formula will not be repeated here: see [21] if needed. For numerical reasons, the center point should be chosen to avoid transforming any points within the spherical triangle to the point at infinity on the Riemann sphere. That can be the centroid of the triangle, or (for triangles less than a hemisphere) any vertex of the triangle.

A Möbius transformation is a function of the form

$$M(z) = \frac{az + b}{cz + d} \tag{23}$$

where a, b, c, d are complex numbers such that $ad - bc \neq 0$. Note the similarity between this function and the homographies mentioned earlier: a Möbius transformation is in fact a homography of the Riemann sphere, although on the Riemann sphere that means that circles and lines are mapped to circles and lines. (Some lines may be mapped to circles, or vice versa.) The inverse of $M(z)$ is $M^{-1}(z) = \frac{dz - b}{-cz + a}$. A Möbius transformation may be specified by the transformation of three complex numbers z_1, z_2, z_3 to $\zeta_1, \zeta_2, \zeta_3$. Assuming all of these values are finite, the Möbius transformation has coefficients as so:

$$a = \det \begin{pmatrix} z_1\zeta_1 & \zeta_1 & 1 \\ z_2\zeta_2 & \zeta_2 & 1 \\ z_3\zeta_3 & \zeta_3 & 1 \end{pmatrix}, b = \det \begin{pmatrix} z_1\zeta_1 & z_1 & \zeta_1 \\ z_2\zeta_2 & z_2 & \zeta_2 \\ z_3\zeta_3 & z_3 & \zeta_3 \end{pmatrix}, c = \det \begin{pmatrix} z_1 & \zeta_1 & 1 \\ z_2 & \zeta_2 & 1 \\ z_3 & \zeta_3 & 1 \end{pmatrix}, d = \det \begin{pmatrix} z_1\zeta_1 & z_1 & 1 \\ z_2\zeta_2 & z_2 & 1 \\ z_3\zeta_3 & z_3 & 1 \end{pmatrix} \tag{24}$$

The Schwarz triangle function conformally transforms the upper half-plane to a triangle whose edges are circular arcs. It is given by:

$$\varphi(\alpha, \beta, \gamma; z) = z^{1-c} \frac{{}_2F_1(a', b'; c'; z)}{{}_2F_1(a, b; c; z)} \tag{25}$$

where ${}_2F_1(a, b; c; z)$ is the hypergeometric function and

$$\begin{aligned} a &= \frac{1-\alpha+\beta-\gamma}{2} \\ b &= \frac{1-\alpha-\beta-\gamma}{2} \\ c &= 1-\alpha \\ a' &= \frac{1+\alpha+\beta-\gamma}{2} = 1+a-c \\ b' &= \frac{1+\alpha-\beta-\gamma}{2} = 1+b-c \\ c' &= 1+\alpha \end{aligned} \tag{26}$$

and the angles at each vertex of the triangle are $\pi\alpha, \pi\beta, \pi\gamma$. (The angles may be dropped if clear in context.) If $\alpha + \beta + \gamma < 1$, then the triangle is hyperbolic; if $= 1$ it is Euclidean, and if > 1 it is spherical.[14] In this text, the hyperbolic case is not relevant.

The Schwarz triangle map maps the boundary of the half-plane (i.e. $\mathbb{R} \cup \{\infty\}$, the real projective line) to the boundary of the triangle. The vertices are the points $z = 0$, 1, and ∞ on that line. The map takes $z = 0$ to 0, $z = 1$ to $\varphi(1) = \frac{\Gamma(c-a)\Gamma(c-b)\Gamma(2-c)}{\Gamma(1-a)\Gamma(1-b)\Gamma(c)}$, and $z = \infty$ to $\varphi(\infty) = \exp(i\pi\alpha) \frac{\Gamma(b)\Gamma(c-a)\Gamma(2-c)}{\Gamma(c)\Gamma(b-c+1)\Gamma(1-a)}$ unless $b = 0$ (the Euclidean case), then $\varphi(\infty) = \exp(i\pi\alpha) \frac{\Gamma(a)\Gamma(2-c)}{\Gamma(a-c+1)}$

No closed-form inverse $\varphi^{-1}(z)$ exists in general, even in the Euclidean case when $b = 0$ and the denominator of $\varphi(z)$ is 1. The function has branch cuts on $(-\infty, 0]$ and $[1, \infty)$, and points are transformed to arbitrarily large values, so care must be taken performing the numerical inversion. A Möbius transformation can be used to estimate initial conditions. The unruliness of this numerical inversion makes it difficult to use in real applications

What remains is to combine all these steps into a conformal map projection between a Euclidean triangle and a spherical triangle. This is also expressed with $\varphi(z)$.

$$\begin{aligned} \zeta &= L(\varphi\left(\alpha_e, \beta_e, \gamma_e; \varphi^{-1}\left(\alpha_s, \beta_s, \gamma_s; M(S(\hat{\mathbf{v}}_0; \hat{\mathbf{v}}))\right)\right) \\ \hat{v} &= S^{-1}\left(\hat{\mathbf{v}}_0; M^{-1}\left(\varphi\left(\alpha_s, \beta_s, \gamma_s; \varphi\left(\alpha_e, \beta_e, \gamma_e; L^{-1}(\zeta)\right)\right)\right)\right) \end{aligned} \tag{27}$$

where $\alpha_s, \beta_s, \gamma_s$ denotes the angles of the spherical triangle (over π), and $\alpha_e, \beta_e, \gamma_e$ denotes the angles of the Euclidean triangle. M is chosen to map $S(\hat{v}_1)$ to 0, $S(\hat{v}_2)$ to $\varphi(\alpha_s, \beta_s, \gamma_s; 1)$, and $S(\hat{v}_3)$ to $\varphi(\alpha_s, \beta_s, \gamma_s; \infty)$. L is a conformal affine transformation, chosen to map 0 to ζ_1, $\varphi(\alpha_e, \beta_e, \gamma_e; 1)$ to ζ_2, and $\varphi(\alpha_e, \beta_e, \gamma_e; \infty)$ to ζ_3. (Only two of these correspondences are needed to determine L.) In complex terms, $L(z) = az + b$, where a and b are complex constants.

The values on the boundary of the triangle depend on the shape of the entire triangle. These values are only guaranteed to be equal on the edge between two triangles if those triangles are reflections of each other across that edge. That is, those triangles are part of a tiling of the sphere with Schwarz triangles.

Deriving a general conformal map projection for quadrilaterals and higher polygons is difficult. While there is only one solution for triangles, for quadrilaterals there is a one-parameter family of solutions, a two-parameter for pentagons, and so forth.[13] Furthermore, except for a few specific cases, the general solution is not a named function: notable exceptions are the elliptic integral and Jacobi elliptic functions, which appear in the functions between the square and the hemisphere.[5] One possible way to handle higher polygons is to divide them into triangles, but a) if new vertices are introduced, those vertices are singular points, and b) those triangles must be Schwarz triangles as mentioned above.

3.3. **Snyder equal-area.** The Snyder equal-area projection can be applied to any regular polygon. The equations in [22] are lengthy, and don't seem to simplify much when expressed in terms of vectors. The special cases of the hemisphere and the cube face do have nice simple forms, however.[12][17] Snyder's equations won't be repeated here.

The Snyder projection starts by subdividing a regular polygonal face into isosceles triangles, where two vertices of the new triangles are vertices of the original polygon, and the third is the center of the polygon. Because of this interruption, the projection is not differentiable on the lines from the center to the original vertices. This projection can be applied to faces larger than a hemisphere, as long as each subdivision triangle is smaller than a hemisphere.

The Snyder projection does not require the faces of a polyhedron to be the same, but does require (to maintain the equal-area property between subdivsions) that the faces be subdividable into identical triangles. In general, the Snyder equal-area projection cannot be adapted to irregular polygons while maintaining the equal-area property and not introducing extra lines of interruption. However, if a polyhedra is made up of identical isosceles triangles, and those triangles meet at appropriate edges, the map can be applied directly to those faces without subdivision. (Isosceles triangles of different dimensions may be allowed if one is willing to abandon either the equal-area property holding between different faces or the polygons on the plane fitting together into a net.) An example of an irregular polyhedra that can be used in this way is an n-bipyramid, formed by gluing two n-sided pyramids together at the n-gonal base. (This is effectively the same as applying the subdivision method to a n-dihedron.) Other polyhedra would include the (regular) icosahedron and octahedron and the tetragonal disphenoid (a stretched form of a tetrahedron with isosceles faces, of which the regular tetrahedron is a subtype).

3.4. **Spherical areal (Triangles).** This projection is an analogy with the relationship of barycentric coordinates to area. Treat β_i as the proportion of spherical area in the triangle that is opposite the vertex $\hat{\mathbf{v}}_i$. Let Ω be the spherical area (solid angle) of the spherical triangle and $\Omega_i = \beta_i \Omega$ be the area of the smaller triangle opposite vertex $\hat{\mathbf{v}}_i$. This area can be found in terms of vectors using this formula:[24][3]

$$\tan(\Omega/2) = \frac{|\hat{\mathbf{v}}_1 \cdot \hat{\mathbf{v}}_2 \times \hat{\mathbf{v}}_3|}{1 + \hat{\mathbf{v}}_1 \cdot \hat{\mathbf{v}}_2 + \hat{\mathbf{v}}_2 \cdot \hat{\mathbf{v}}_3 + \hat{\mathbf{v}}_3 \cdot \hat{\mathbf{v}}_1} \tag{28}$$

The formula to find $\hat{\mathbf{v}}$ given β_i more complicated, although it's also derived from the formula for spherical area.

$$\begin{aligned}
\mathbf{G}\hat{\mathbf{v}} &= \mathbf{h} \\
\mathbf{G} &= \begin{bmatrix}\mathbf{g}_1 & \mathbf{g}_2 & \mathbf{g}_3\end{bmatrix} \\
\mathbf{h} &= \begin{bmatrix}h_1 & h_2 & h_3\end{bmatrix}^T \\
\mathbf{g}_i &= (1 + \cos\Omega_i)\,\mathbf{v}_{i-1} \times \mathbf{v}_{i+1} - \sin\Omega_i\,(\mathbf{v}_{i-1} + \mathbf{v}_{i+1}) \\
h_i &= \sin\Omega_i\,(1 + \mathbf{v}_{i-1} \cdot \mathbf{v}_{i+1})
\end{aligned} \tag{29}$$

The subscripts loop around: 0 should be interpreted as 3, and 4 should be interpreted as 1. To clarify, $\mathbf{G}$ is the 3x3 matrix where the ith column is $\mathbf{g}_i$, and $\mathbf{h}$ is the column vector where the ith element is h_i. The vector $\hat{\mathbf{v}}$ can be solved for using standard matrix methods.

OR:

$$\begin{aligned}
\tau &= \tan\left(\frac{\Omega}{2}\right) \\
\tau_i &= \tan\left(\frac{\Omega_i}{2}\right) \\
t_i &= \frac{\tau_i}{\tau} \\
a_i &= \mathbf{v}_{i-1} \cdot \mathbf{v}_{i+1} \\
b_i &= \frac{a_{i-1} + a_{i+1}}{1 + a_i} \\
c_i &= \frac{t_i}{(1 + b_i) + (1 - b_i)t_i} \\
f_i &= \frac{c_i}{1 - c_1 - c_2 - c_3} \\
\mathbf{v} &= \sum f_i \mathbf{v}_i = \frac{\sum c_i \mathbf{v}_i}{1 - \sum c_i}
\end{aligned} \tag{30}$$

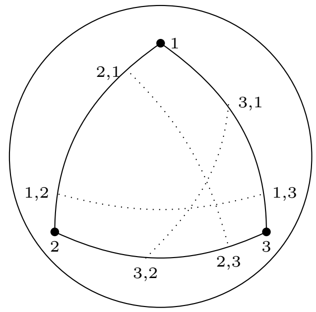

FIGURE 5. Intersection of great circle arcs inside a spherical triangle, and the small spherical triangle formed by the arcs. Exaggerated so that the small triangle is visible; not to scale.

3.5. **Fuller.** note similiarities between chamberlin and fuller, as per [9]

This is Method 2 in geodesic dome terminology. Recall in our earlier discussion of barycentric coordinates that on a plane triangle, we can draw a line corresponding to each β_i, and those three lines meet at a point. On the sphere, if we make the same construction, the lines do not meet at a point (except on the edges), but instead intersect to form a small spherical triangle. Take a point within that triangle as $\mathbf{v}$. Typically the centroid is used, as it's easy to calculate, although we'll discuss another variation.

(If there were any ambiguities, we used the program `geodesic` from Antiprism[19] as a reference implementation.)

In analytic terms, use Slerp to determine the points on each triangle edge. Take the cross product of the opposing pairs of points to determine the normal to the intersecting plane corresponding to each line. Take the cross product of each pair of normals to find a vector proportional to the point of intersection. (As the cross product is antisymmetric, be careful about order here.) Then normalize each vector and take their centroid.

In terms of equations, Method 2 or the Great Circle Intersection method on a triangle is:

$$\begin{aligned} \tilde{\mathbf{v}} &= \sum_{i=1}^{3} \frac{\mathbf{h}_i \times \mathbf{h}_{i+1}}{\|\mathbf{h}_i \times \mathbf{h}_{i+1}\|} \\ \mathbf{h}_i &= \mathrm{Slerp}(\mathbf{v}_{i-1}, \mathbf{v}_i; \beta_i) \times \mathrm{Slerp}(\mathbf{v}_{i+1}, \mathbf{v}_i; \beta_i) \end{aligned} \tag{31}$$

No explicit inverse, unlike [10][2]

The above equation can be tweaked slightly by removing the step of normalizing the vectors at the points of intersection. This still produces a point within the triangle. This formula is a little more computationally efficient and easier to treat algebraically. Where $\mathbf{h}_i$ is as before:

$$\tilde{\mathbf{v}} = \sum_{i=1}^{3} \mathbf{h}_i \times \mathbf{h}_{i+1} \tag{32}$$

This method can be extended to the Quadrilateral. Use Slerp to find points on opposing sides of the quadrilateral, use the cross product to find their normal, and then use the cross product to find the point of intersection. Since we draw two intersecting lines, there is only one point of intersection within the quadrilateral. The formula is:

$$\tilde{\mathbf{v}} = (\mathrm{Slerp}(\mathbf{v}_1, \mathbf{v}_2; \frac{u+1}{2}) \times \mathrm{Slerp}(\mathbf{v}_4, \mathbf{v}_3; \frac{u+1}{2})) \times (\mathrm{Slerp}(\mathbf{v}_1, \mathbf{v}_4; \frac{v+1}{2}) \times \mathrm{Slerp}(\mathbf{v}_2, \mathbf{v}_3; \frac{v+1}{2})) \tag{33}$$

This is similar to the Great Circle method, except instead of using the great circles to calculate the intersections of the lines, we use another spherical linear interpolation to get a point near the intersection. We effectively use the Lerp formulas from the section on coordinates, substituting Slerp for Lerp. Unlike Lerp, Slerp does not commute, so we take the different permutations of the arguments and combine the different points that result.

Triangular:

$$\widetilde{\mathbf{v}} = \sum_{i=3}^{3} \operatorname{Slerp}(\operatorname{Slerp}(\mathbf{v}_{i-1}, \mathbf{v}_i; \beta_i), \operatorname{Slerp}(\mathbf{v}_{i+1}, \mathbf{v}_i; \beta_i); \frac{\beta_{i-1}}{1-\beta i}) \tag{34}$$

Quadrilateral:

$$\begin{aligned} \widetilde{\mathbf{v}} =& \operatorname{Slerp}(\operatorname{Slerp}(\mathbf{v}_1, \mathbf{v}_2; \frac{u+1}{2}), \operatorname{Slerp}(\mathbf{v}_4, \mathbf{v}_3; \frac{u+1}{2}); \frac{v+1}{2}) \\ &+ \operatorname{Slerp}(\operatorname{Slerp}(\mathbf{v}_1, \mathbf{v}_4; \frac{v+1}{2}), \operatorname{Slerp}(\mathbf{v}_2, \mathbf{v}_3; \frac{v+1}{2}); \frac{u+1}{2}) \end{aligned} \tag{35}$$

(or is this forward fuller and the other one's reverse fuller?)
Solve for each β_i':

$$\begin{vmatrix} \mathbf{v} & \operatorname{Slerp}(\mathbf{v}_{i-1}, \mathbf{v}_i; \beta_i') & \operatorname{Slerp}(\mathbf{v}_{i+1}, \mathbf{v}_i; \beta_i') \end{vmatrix} = 0 \tag{36}$$

β_i does not have a closed-form solution on general triangles, but each β_i can be optimized separately, so the optimization process is not too unwieldy.

In general, $\sum \beta_i' \neq 1$ for the β_i' resulting from this process. Let $\beta_i = \frac{\beta_i'}{\sum \beta_i}$.
(square) Solve for u, v:

$$\begin{aligned} \begin{vmatrix} \mathbf{v} & \operatorname{Slerp}(\mathbf{v}_1, \mathbf{v}_2; \tfrac{u+1}{2}) & \operatorname{Slerp}(\mathbf{v}_4, \mathbf{v}_3; \tfrac{u+1}{2}) \end{vmatrix} = 0 \\ \begin{vmatrix} \mathbf{v} & \operatorname{Slerp}(\mathbf{v}_1, \mathbf{v}_4; \tfrac{v+1}{2}) & \operatorname{Slerp}(\mathbf{v}_2, \mathbf{v}_3; \tfrac{v+1}{2}) \end{vmatrix} = 0 \end{aligned} \tag{37}$$

For each i, solve for β_{i-1} and βi. Average the results.

$$\mathbf{v} = \operatorname{Slerp}(\mathbf{v}_{i-1}, \mathbf{v}_i; \beta_i), \operatorname{Slerp}(\mathbf{v}_{i+1}, \mathbf{v}_i; \beta_i); \frac{\beta_{i-1}}{1-\beta i}) \tag{38}$$

Solve for u, v:

$$\begin{aligned} \mathbf{v} =& \operatorname{Slerp}(\operatorname{Slerp}(\mathbf{v}_1, \mathbf{v}_2; \frac{u+1}{2}), \operatorname{Slerp}(\mathbf{v}_4, \mathbf{v}_3; \frac{u+1}{2}); \frac{v+1}{2}) \\ \mathbf{v} =& \operatorname{Slerp}(\operatorname{Slerp}(\mathbf{v}_1, \mathbf{v}_4; \frac{v+1}{2}), \operatorname{Slerp}(\mathbf{v}_2, \mathbf{v}_3; \frac{v+1}{2}); \frac{u+1}{2}) \end{aligned} \tag{39}$$

3.6. **Naive Slerp.** The Naive Slerp method is derived by a naive analogy with spherical linear interpolation (Slerp) extended to barycentric or uv coordinates, thus the name.

3.6.1. *Triangles.*

$$\widetilde{\mathbf{v}} = \sum_{i=1}^{3} \frac{\sin(w\beta_i)}{\sin(w)} \mathbf{v}_i \tag{40}$$

Here, w is a function of β_i. Let w_i be the spherical length of the edge opposite vertex i. Then,

$$w = \frac{\beta_0\beta_1 w_2 + \beta_1\beta_2 w_0 + \beta_2\beta_0 w_1}{\beta_0\beta_1 + \beta_1\beta_2 + \beta_2\beta_0}. \tag{41}$$

This function satisfies the requirement that $w = w_i$ on the edge opposite vertex i, and elsewhere on the triangle smoothly parameterizes between the values. w is not defined at the vertices, and does not have a limit there unless the two edges that meet at that vertex have the same length. However, any positive value for w can be used there without changing the result. If all the edges are equal length, w can be replaced with that constant edge length.

3.6.2. *Quadrilaterals.* These are two functions that can be derived by analogy with uv coordinates. Let w_{ij} be the spherical length of the edge between vertices i and j. One:

$$
\begin{aligned}
\widetilde{\mathbf{v}} &= \sum_{i=1}^{4} \frac{s_i}{\sin(w_u)\sin(w_v)} \mathbf{v}_i \\
s_1 &= \sin\left(w_u \frac{1-u}{2}\right) \sin\left(w_v \frac{1-v}{2}\right) \\
s_2 &= \sin\left(w_u \frac{1+u}{2}\right) \sin\left(w_v \frac{1-v}{2}\right) \\
s_3 &= \sin\left(w_u \frac{1+u}{2}\right) \sin\left(w_v \frac{1+v}{2}\right) \\
s_4 &= \sin\left(w_u \frac{1-u}{2}\right) \sin\left(w_v \frac{1+v}{2}\right)
\end{aligned} \tag{42}
$$

where

$$
\begin{aligned}
w_u &= (1-v)w_{12} + (1+v)w_{34}, \\
w_v &= (1-u)w_{23} + (1+u)w_{14}
\end{aligned} \tag{43}
$$

Unlike before, the interpolations of w_u and w_v do not have undefined points. However, they may cause undefined values in the mapping if there is a point where one is equal to zero.

Two:

$$
\begin{aligned}
\widetilde{\mathbf{v}} &= \sum_{i=1}^{4} \frac{\sin(w\gamma_i)}{\sin(w)} \mathbf{v}_i \\
\gamma_1 &= \frac{(1-u)(1-v)}{4} \\
\gamma_2 &= \frac{(1+u)(1-v)}{4} \\
\gamma_3 &= \frac{(1+u)(1+v)}{4} \\
\gamma_4 &= \frac{(1-u)(1+v)}{4}
\end{aligned} \tag{44}
$$

where

$$
\begin{aligned}
w &= \frac{t_{12}w_{12} + t_{23}w_{23} + t_{34}w_{34} + t_{41}w_{41}}{t_{12} + t_{23} + t_{34} + t_{41}} \\
t_{12} &= (1-u)(1-v)(1+u) \\
t_{23} &= (1-v)(1+u)(1+v) \\
t_{34} &= (1-u)(1+u)(1+v) \\
t_{41} &= (1-u)(1-v)(1+v)
\end{aligned} \tag{45}
$$

Again, this expression is undefined at the vertices, but can be replaced with any positive value there. If all the edges are equal length, w can be replaced with that constant edge length.

3.6.3. *Projection of* $\widetilde{\mathbf{v}}$. The naive slerp methods produces unit vectors along the edges. Because the projected edges already lie on the sphere, we have freedom in how to adjust $\widetilde{\mathbf{v}}$ to lie on the sphere. The easiest is just to centrally project the vertices, that is, to normalize $\widetilde{\mathbf{v}}$ like we have been. Another option is to perform a parallel projection along the face normal, as defined earlier. We need the parallel distance p from the vertex to the sphere surface in the direction of the face normal $\hat{\mathbf{n}}$, such that $\hat{\mathbf{v}} = \widetilde{\mathbf{v}} + p\hat{\mathbf{n}}$. p is given by:

$$
p = -\widetilde{\mathbf{v}} \cdot \hat{\mathbf{n}} + \sqrt{1 + \widetilde{\mathbf{v}} \cdot \hat{\mathbf{n}} - \widetilde{\mathbf{v}} \cdot \widetilde{\mathbf{v}}} \tag{46}
$$

p can also be approximated as $\widetilde{p} = 1 - \|\widetilde{\mathbf{v}}\| \leq p$, which takes fewer operations and doesn't require calculation of the face normal. Technically, you can project in almost any direction, not just that of the face normal, but most other choices don't produce a symmetric result.

Really, the projection can be performed from any point in space. Central projection uses rays from a point at the center of the sphere, and parallel can be thought of as using rays from a point at infinity. Instead of specifying the point, we define a linear combination of the two projections:

$$\hat{\mathbf{v}} = \frac{\widetilde{\mathbf{v}} + kp\mathbf{c}}{\|\cdots\|} \tag{47}$$

When $k = 0$, that's the central projection: when $k = 1$, it's the parallel projection. p may be replaced by $\widetilde{p}$. If our goal is to optimize a measurement of the map projection, like conformality or area distortion, we can do a 1-variable optimization on k.

3.6.4. *Spherical rectangle.* Naive slerp 1 simplifies nicely for some particular spherical rectangles and squares. Let the target rectangle be defined by the points $(-a, -b, c)$, $(a, -b, c)$, (a, b, c), and $(-a, b, c)$ where a, b, c are in $[0, 1]$ and $a^2 + b^2 + c^2 = 1$. The spherical center of this rectangle, and the face normal, is $(0, 0, 1)$. Naive slerp 1 from the standard square to this rectangle is expressible as so:

$$\begin{aligned}
\widetilde{x} &= \frac{\sin(\frac{w_u}{2}u)\cos(\frac{w_v}{2}v)}{\sqrt{1-b^2}} \\
\widetilde{y} &= \frac{\cos(\frac{w_u}{2}u)\sin(\frac{w_v}{2}v)}{\sqrt{1-a^2}} \\
\widetilde{z} &= \frac{c}{\sqrt{1-a^2}\sqrt{1-b^2}}\cos(\frac{w_u}{2}u)\cos(\frac{w_v}{2}v)
\end{aligned} \tag{48}$$

where $cos(w_u) = 1 - 2a^2$ and $cos(w_v) = 1 - 2b^2$.

In the case where $a = b$, denote $w = w_u = w_v$, so the above can be expressed as:

$$\begin{aligned}
\widetilde{x} &= \frac{\sin\left(\frac{w}{2}(u+v)\right) + \sin\left(\frac{w}{2}(u-v)\right)}{2\sqrt{1-a^2}} \\
\widetilde{y} &= \frac{\sin\left(\frac{w}{2}(u+v)\right) - \sin\left(\frac{w}{2}(u-v)\right)}{2\sqrt{1-a^2}} \\
\widetilde{z} &= \frac{c}{2-2a^2}\left(\cos\left(\frac{w}{2}(u+v)\right) + \cos\left(\frac{w}{2}(u-v)\right)\right)
\end{aligned} \tag{49}$$

which demonstrates that this mapping on this polygon preserves diagonal lines.

In the case when $c = 0$, and the spherical rectangle takes up an entire hemisphere, the formula further reduces to:

$$\begin{aligned}
\widetilde{x} &= \frac{\sin(\frac{w_x}{2}u)\cos(\frac{w_y}{2}v)}{a} \\
\widetilde{y} &= \frac{\cos(\frac{w_x}{2}u)\sin(\frac{w_y}{2}v)}{b} \\
\widetilde{z} &= 0
\end{aligned} \tag{50}$$

In the limit where $c = 0$ and $b = 0$,

$$\begin{aligned}
\widetilde{x} &= \sin(\frac{\pi}{2}u) \\
\widetilde{y} &= v\cos(\frac{\pi}{2}u) \\
\widetilde{z} &= 0
\end{aligned} \tag{51}$$

3.7. **Elliptical.** This quadrilateral map is based on naive slerp 1 on a spherical rectangle, as described in the previous section. Let the vertices of the rectangle be defined as before.

$\sin(kx)$ may be approximated as $\sin(k)x$, where the two expressions are equal at $x = -1, 0, 1$. Similarly, $\cos(kx)$ may be approximated as $\sqrt{1 - \sin^2(k)x^2}$. This approximation was applied in [18] to produce an approximate equal-area homeomorphism, as it maintains the boundary of the shape where $x = \pm 1$ or $y = \pm 1$. Applying this approximation to the equation for naive slerp on a spherical rectangle yields:

$$\begin{aligned}\widetilde{x} &= au\frac{\sqrt{1-b^2v^2}}{\sqrt{1-b^2}}\\ \widetilde{y} &= bv\frac{\sqrt{1-a^2u^2}}{\sqrt{1-a^2}}\\ \widetilde{z} &= c\frac{\sqrt{1-a^2u^2}\sqrt{1-b^2v^2}}{\sqrt{1-a^2}\sqrt{1-b^2}}\end{aligned} \tag{52}$$

In the case when $c = 0$, and the spherical rectangle takes up an entire hemisphere, the formula reduces to:

$$\begin{aligned}\widetilde{x} &= u\sqrt{1-b^2v^2}\\ \widetilde{y} &= v\sqrt{1-a^2u^2}\\ \widetilde{z} &= 0\end{aligned} \tag{53}$$

When $a = b = \frac{1}{\sqrt{2}}$, this is the Nowell's elliptical function from the square to the disk.[15][6] Furthermore, when $c = b = 0$,

$$\begin{aligned}\widetilde{x} &= u\\ \widetilde{y} &= v\sqrt{1-u^2}\\ \widetilde{z} &= 0\end{aligned} \tag{54}$$

which is the "squelch" function from the square to the disk in [6].

3.8. **Grid-based.**

3.8.1. *Inversion.*

3.8.2. *Repeated subdivision.* Method 3 in geodesic dome terms

4. Analysis

4.1. **From the sphere to the plane.**

4.2. **From the plane to the sphere.**

5. Conclusion

References

[1] FK Chan and EM O'Neill. Feasibility study of a quadrilateralized spherical cube earth data base. Technical report, Environmental Prediction Research Facility Tech. Rep., 2-75 (CSC), 1975.
[2] John E Crider. Exact equations for fuller's map projection and inverse. *Cartographica: The International Journal for Geographic Information and Geovisualization*, 43(1):67–72, 2008.
[3] Folke Eriksson. On the measure of solid angles. *Mathematics Magazine*, 63(3):184–187, 1990. doi:10.2307/2691141. JSTOR 2691141.
[4] Chamberlain Fong. Analytical methods for squaring the disc. *arXiv preprint arXiv:1509.06344*, 2015.
[5] Chamberlain Fong. The conformal hyperbolic square and its ilk. In *Bridges Conference Proceedings*, pages 9–13, 2016.
[6] Chamberlain Fong. Elliptification of rectangular imagery. *arXiv preprint arXiv:1709.07875*, 2017.
[7] Chamberlain Fong. Homeomorphisms between the circular disc and the square. *Handbook of the Mathematics of the Arts and Sciences*, pages 1–26, 2018.
[8] Kenneth Gade. A non-singular horizontal position representation. *The journal of navigation*, 63(3):395–417, 2010. doi:10.1017/S0373463309990415.

[9] Robert W Gray. Fuller's dymaxion$^{\mathrm{TM}}$ map. *Cartography and Geographic Information Systems*, 21(4):243–246, 1994.

[10] Robert W Gray. Exact transformation equations for fuller's world map. *Cartographica: The International Journal for Geographic Information and Geovisualization*, 32(3):17–25, 1995.

[11] Hugh Kenner. *Geodesic math and how to use it.* Univ of California Press, 1976.

[12] Martin Lambers. Mappings between sphere, disc, and square. *Journal of Computer Graphics Techniques Vol*, 5(2), 2016.

[13] Zeev Nehari. Domains bounded by circular arcs. In *Conformal Mapping*, chapter 5.7, pages 198–208. Dover, 1975.

[14] Zeev Nehari. The schwarzian s-functions. In *Conformal Mapping*, chapter 6.5, pages 308–317. Dover, 1975.

[15] Philip Nowell. Mapping a square to a circle. http://mathproofs.blogspot.com/2005/07/mapping-square-to-circle.html, 2005. Accessed: 2019-03-03.

[16] EM O'Neill and RE Laubscher. Extended studies of a quadrilateralized spherical cube earth data base. Technical report, Naval Environmental Prediction Research Facility Tech. Rep., 3-76 (CSC), 1976.

[17] Fred Patt. Comments on draft wcs standard. http://www.sai.msu.su/ megera/wiki/SphereCube, 1993.

[18] Marc B Reynolds. Square/disc mappings. http://marc-b-reynolds.github.io/math/2017/01/08/SquareDisc.html. Accessed: 2019-05-16.

[19] Adrian Rossiter. *Antiprism*, 2018. http://www.antiprism.com/.

[20] Kevin Sahr and Denis White. Discrete global grid systems. *Computing Science and Statistics*, pages 269–278, 1998.

[21] John P Snyder. *Map projections–A working manual*, volume 1395. US Government Printing Office, 1987.

[22] John P Snyder. An equal-area map projection for polyhedral globes. *Cartographica: The International Journal for Geographic Information and Geovisualization*, 29(1):10–21, 1992.

[23] John Parr Snyder and Philip M Voxland. *An album of map projections.* Number 1453. US Government Printing Office, 1989.

[24] Adriaan Van Oosterom and Jan Strackee. The solid angle of a plane triangle. *IEEE transactions on Biomedical Engineering*, 30(2):125–126, 1983.

Appendix A. The Chamberlin Trimetric Projection